

C. elegans *daf-6* Encodes a Patched-Related Protein Required for Lumen Formation

Elliot A. Perens and Shai Shaham*
Laboratory of Developmental Genetics
The Rockefeller University
1230 York Avenue
New York, New York 10021

Summary

Sensory organs are often composed of neuronal sensory endings accommodated in a lumen formed by ensheathing epithelia or glia. Here we show that lumen formation in the *C. elegans* amphid sensory organ requires the gene *daf-6*. *daf-6* encodes a Patched-related protein that localizes to the luminal surfaces of the amphid channel and other *C. elegans* tubes. While *daf-6* mutants display only amphid lumen defects, animals defective for both *daf-6* and the *Dispatched* gene *che-14* exhibit defects in all tubular structures that express *daf-6*. Furthermore, DAF-6 protein is mislocalized, and lumen morphogenesis is abnormal, in mutants with defective sensory neuron endings. We propose that amphid lumen morphogenesis is coordinated by neuron-derived cues and a DAF-6/CHE-14 system that regulates vesicle dynamics during tubulogenesis.

Introduction

Sensory structures in many organisms share a common morphology in which sensory neuron endings extend through a tubular channel formed by their associated glia or epithelia (Ward et al., 1975; Burkitt et al., 1993; Jan and Jan, 1993). The formation of all biological tubes, both unicellular and multicellular, has been proposed to occur by a common mechanism in which vesicles within the tube-forming cells coalesce at a luminal surface of apical character (Lubarsky and Krasnow, 2003). This process has been observed in cultured Madin-Darby canine kidney (MDCK) cells (Montesano et al., 1991), capillary-forming endothelial cells (Folkman and Haudenschild, 1980; Davis and Camarillo, 1996), *Drosophila* salivary glands (Myat and Andrew, 2002), and the *C. elegans* excretory canal cell (Berry et al., 2003). Some of the molecular players controlling tube outgrowth and branching are known (Ghabrial et al., 2003); however, the initial steps of lumen formation and morphogenesis are poorly understood. Glia that ensheath sensory neuron endings or myelinate neuronal projections must regulate their lumen dimensions to accommodate precisely their resident neuronal processes. Little is known about how this is accomplished (Wegner, 2000), although it is reasonable to hypothesize that neuronal processes induce aspects of glial lumen formation.

To understand sensory organ morphogenesis and specifically glial lumen formation, we have been study-

ing the *C. elegans* amphid sensory organ. *C. elegans* possesses two bilaterally symmetric amphids at the anterior tip of the animal (Ward et al., 1975). Each amphid consists of 12 sensory neurons and 2 ensheathing glial cells, the sheath and socket cells. Amphid neurons have two projections: an axon that extends into the nerve ring and a dendrite that extends to the anterior tip of the animal. Amphid sheath and socket glia also extend anterior processes that contact amphid neuron dendritic projections (Ward et al., 1975). At the tip of the nose, all neuronal sensory endings are ensheathed by the sheath glia (Figures 1A and 1B). Four of the amphid neurons, which mediate chemotaxis to volatile chemicals and thermotaxis (Bargmann et al., 1993; Mori and Ohshima, 1995), have dendritic endings that are fully embedded within the amphid sheath glia. The remaining eight neurons end in sensory cilia that access the outside environment by extending through a matrix-filled amphid channel: a bipartite channel, formed anteriorly by the socket cell and continued posteriorly by the sheath cell (Figure 1B; Ward et al., 1975). We will henceforth refer to this channel as the amphid channel. Amphid channel neurons are required for avoidance of high osmolarity solutions, chemosensation of water-soluble solutes, mechanosensation, and sensation of dauer pheromone (Bargmann and Mori, 1997; Driscoll and Kaplan, 1997; Riddle and Albert, 1997).

Animals defective in the *daf-6* gene (*daf*, dauer formation defective) were first isolated because of their inability to enter an alternative developmental state known as dauer (Riddle et al., 1981). Entry into dauer is mediated by a continuously released pheromone (Riddle and Albert, 1997). Four previous observations suggest that *daf-6* mutants have amphid channel defects. First, *daf-6* mutants are defective in sensory functions that require direct exposure of channel neurons to the outside environment (Albert et al., 1981; Perkins et al., 1986) but respond normally to volatile odorants, temperature changes, and mechanosensory stimuli (Albert et al., 1981; Bargmann et al., 1993; Perkins et al., 1986) that do not require direct access to the animal's surroundings. Second, in wild-type animals, channel neurons can take up lipophilic dyes such as DiO from the environment (Hedgecock et al., 1985); however, *daf-6* mutants are dye-filling defective (Starich et al., 1995). Third, Herman (1987) demonstrated by mosaic analysis that *daf-6* function is required in the amphid sheath glia and not in the amphid neurons for dye uptake. Fourth, using scanning electron microscopy, an open channel could not be found in the anterior tip of the amphid in *daf-6* mutants (Albert et al., 1981).

Here we describe our studies of *daf-6*. We show that the amphid channel fails to open anteriorly in *daf-6* mutants, consistent with a role for *daf-6* in lumen formation. We also demonstrate that *daf-6* function is required in the amphid around the time of lumen formation. *daf-6* encodes a conserved, sterol-sensing domain (SSD)-containing protein related to the vertebrate and *Drosophila* Hedgehog receptor Patched. A rescuing DAF-6::GFP fusion protein localized to the lu-

*Correspondence: shaham@rockefeller.edu

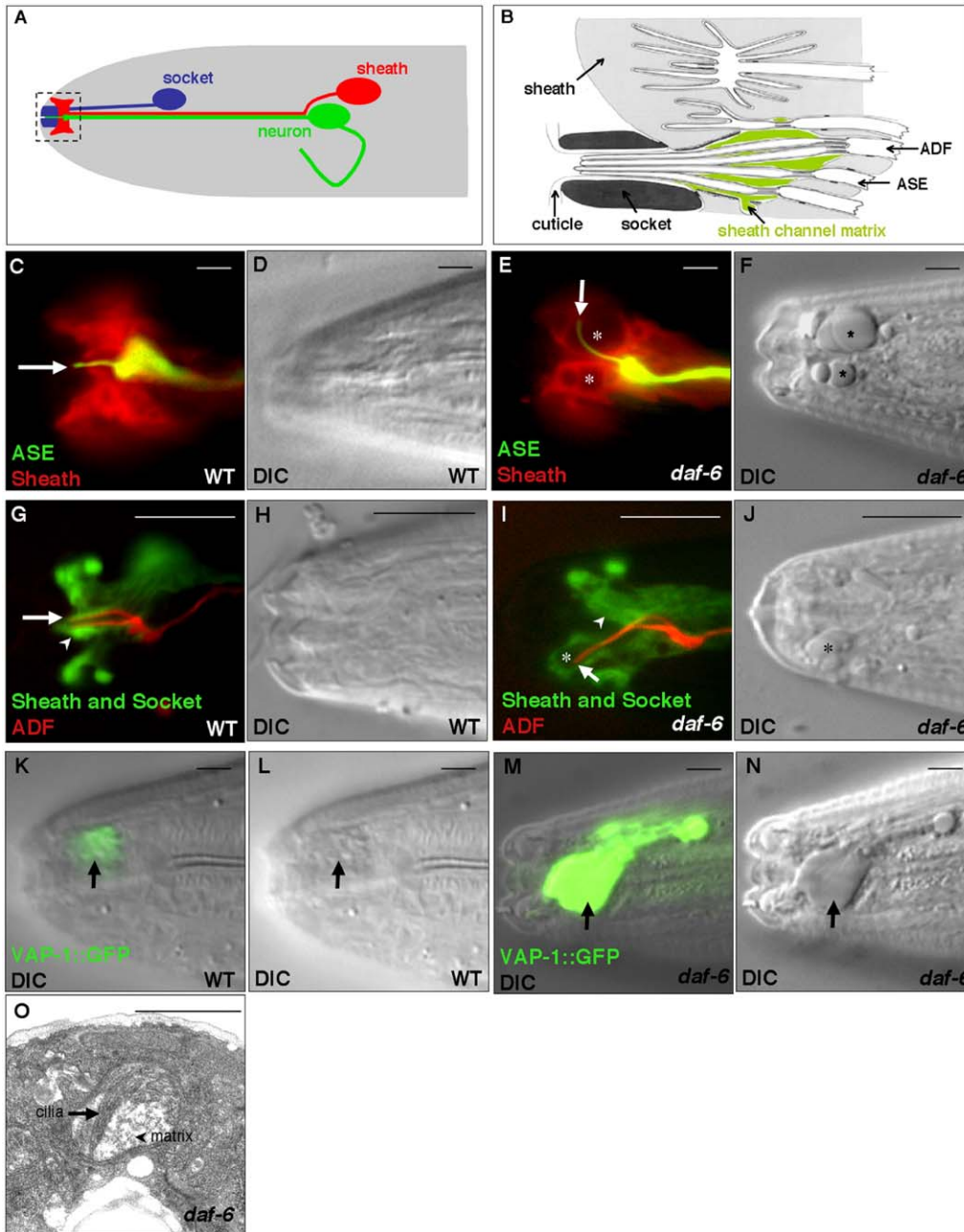


Figure 1. The Amphid Sheath Cell Lumen Fails to Open in *daf-6* Mutants

(A) A schematic of the head region of *C. elegans* depicting the three cell types of an amphid. Boxed region is area seen in (B)–(N).
 (B) A schematic of the anterior end of an amphid (after Perkins et al., 1986). Cilia of ASE and ADF neurons extend through the amphid channel. Green, channel matrix.
 (C and D) Fluorescence image (C) and DIC image (D) of a wild-type adult containing P_{gcy-5} :GFP (ASER) and P_{vap-1} :DsRed (sheath) reporter transgenes. ASE cilium (arrow) extends through sheath cell lumen.
 (E and F) Same as (C) and (D), respectively, except that a *daf-6(e1377)* adult is shown. ASE cilium (arrow) fails to extend through the sheath cell. Asterisks, vacuoles.
 (G and H) Fluorescence image (G) and DIC image (H) of a wild-type L2 containing $P_{T08G3.3}$:DsRed (ADF) and P_{daf-6} :GFP transgenes (socket [arrowhead] and sheath). ADF double cilium (arrow) extends through the sheath channel into the socket channel.
 (I and J) Same as (G) and (H), respectively, except that a *daf-6(e1377)* L2 is shown. ADF cilium (arrow) does not extend through the sheath channel into the socket channel (arrowhead). Asterisk, vacuole.
 (K and L) Merged DIC and fluorescence image (K) and DIC image (L) of a wild-type adult expressing P_{vap-1} :*vap-1::GFP*.
 (M and N) Merged DIC and fluorescence image (M) and DIC image (N) of a *daf-6(e1377)* adult expressing P_{vap-1} :*vap-1::GFP*. Arrows, sheath cell vacuoles.
 (O) Electron micrograph of a section through the amphid of a *daf-6(e1377)* L1. Neuronal cilia, which curve laterally, reside within a sheath pocket containing matrix material.
 (A–N) Anterior is left, dorsal is up. Scale bars equal 5 μ m.
 (O) Scale bar equals 1 μ m.

minial surfaces of several tubular structures, including those of the amphid sheath glia. *daf-6* interacted genetically with the *Dispatched* gene *che-14*, suggesting that both genes function in concert in the same cells to regulate lumen formation in multiple *C. elegans* tubes. Finally, we uncovered a requirement for ciliated endings of amphid sensory neurons in regulating DAF-6 localization and morphogenesis of the amphid channel. Our results provide insights into the genetic basis of tube morphogenesis during sensory organ formation and during tubulogenesis in general. Furthermore, our results demonstrate a dedicated role for a member of a previously uncharacterized subfamily of SSD-containing proteins in lumen formation.

Results

daf-6 Mutants Contain Abnormal Amphid Channels

To understand the cause of the sensory deficits in *daf-6* mutants, we examined the structure of the amphids in these animals. Specifically, we examined animals homozygous for the strong loss-of-function allele *daf-6(e1377)* that harbored a P_{vap-1} -DsRed transgene, expressing DsRed fluorescent protein in amphid sheath glia under control of the *vap-1* gene promoter (*vap*, venom allergen protein; Sutherlin et al., 2001); and a P_{gcy-5} -GFP transgene, expressing green fluorescent protein (GFP) in the right ASE (ASER) amphid channel neuron (Yu et al., 1997). We identified three defects in these animals, all consistent with a failure of the amphid channel to open anteriorly.

First, whereas the sheath channel was open in wild-type animals (Figures 1C and 1D), this portion of the channel was not open in *daf-6(e1377)* animals (Figures 1E and 1F). Consistent with this observation, the ASER neuronal cilia of wild-type animals extended through the sheath channel (Figures 1C and 1D), but the ASER cilia of *daf-6(e1377)* animals did not penetrate the sheath channel (Figures 1E and 1F). A similar defect was observed for the ADF neurons in *daf-6(e1377)* animals (Figures 1G–1J).

Second, whereas wild-type cilia were straight (Figures 1C and 1G), the cilia in *daf-6(e1377)* animals tended to curve near the tip of the nose (Figures 1E and 1I), seemingly in response to the physical constraint of being embedded within the sheath cell.

Third, *daf-6(e1377)* adults contained vacuolar structures within the sheath cell (Figures 1E and 1F) that were not seen in wild-type adults (Figures 1C and 1D). These structures may correspond to the vacuoles seen previously in electron microscope (EM) sections of adult *daf-6(e1377)* animals (Albert et al., 1981). To determine the contents of these abnormal vacuoles, we examined *daf-6(e1377)* animals expressing the VAP-1::GFP protein in the sheath glia. VAP-1 is a component of the sheath glia matrix: an undefined matrix encased in large secretory vesicles that is secreted from the amphid sheath glia into the channel surrounding the sensory cilia (M. Heiman and S.S., unpublished results; Figures 1B, 1K, and 1L; Ward et al., 1975). VAP-1 can be released from animals to their surroundings (Sutherlin et al., 2001), presumably through the amphid channel. As shown in Figures 1M and 1N, VAP-1::GFP accumu-

lated within sheath cell vacuolar structures, suggesting that these vacuoles contained matrix material. Consistent with this observation, EM cross-sections of *daf-6(e1377)* animals revealed that amphid cilia resided within a sheath cell pocket containing material similar in electron density to matrix material (Figure 1O). These findings are also consistent with a failure to open the sheath glia channel: failure in channel opening prevents matrix material from exiting the animal, causing this material to accumulate at the anterior tip of the sheath glia.

Vacuole accumulation and bending of ciliated sensory endings may both be secondary manifestations of the closure of the sheath cell channel in *daf-6(e1377)* animals. If this were true, these defects might not be present early during channel development. Indeed, young *daf-6(e1377)* larvae did not frequently contain bent cilia or vacuolar structures. However, dye uptake was completely blocked at all stages, indicating that channel neurons always lacked access to the outside environment. Furthermore, animals at all stages observed also exhibited fully penetrant defects in cilia extension through the sheath channel into the socket channel (see Supplemental Table S1 available with this article online; Figures 1C–1J).

These studies suggest that failure to generate an open sheath cell channel, and the resulting failure of the amphid cilia to gain exposure to the external environment, are the primary causes of the sensory deficits of *daf-6* mutants.

Sensory defects in *daf-6* mutants could be due not only to structural defects in the amphid channel, but also to defects in the sensory cilia themselves. To determine whether cilia components were misexpressed or mislocalized in *daf-6(e1377)* animals, we examined localization of the cilia resident protein CHE-2 (Fujiwara et al., 1999). Functional CHE-2::GFP protein was localized to amphid cilia in 20/20 *daf-6(e1377)* animals examined, suggesting that at least one cilia component was properly localized in these mutants.

daf-6 Encodes a Patched-Related Protein

To understand how *daf-6* controls amphid channel opening, we cloned the gene. *daf-6* was previously mapped between the *unc-3* and *unc-7* genes on linkage group X (Herman, 1984). We established strains homozygous for the *daf-6(e1377)* allele and containing extrachromosomal arrays of candidate cosmids from the genetic interval described above. The dye-filling defect of *daf-6(e1377)* animals was fully rescued by two extrachromosomal arrays containing cosmid F31F6 (data not shown). A predicted gene in this region, F31F6.5 (also named *ptr-7*; Kuwabara et al., 2000), encodes a protein related to the sterol-sensing domain (SSD)-containing protein Patched. To determine whether *daf-6* is F31F6.5/*ptr-7*, we generated a 9 kb subclone of F31F6 that included 3 kb of sequence upstream of the predicted *ptr-7* ATG, and the full *ptr-7* genomic coding region fused to GFP. Four transmitted lines containing this subclone rescued the dye uptake defect of *daf-6(e1377)* animals as efficiently as the cosmid (data not shown; see below).

To confirm that *daf-6* is F31F6.5/*ptr-7* and to deter-

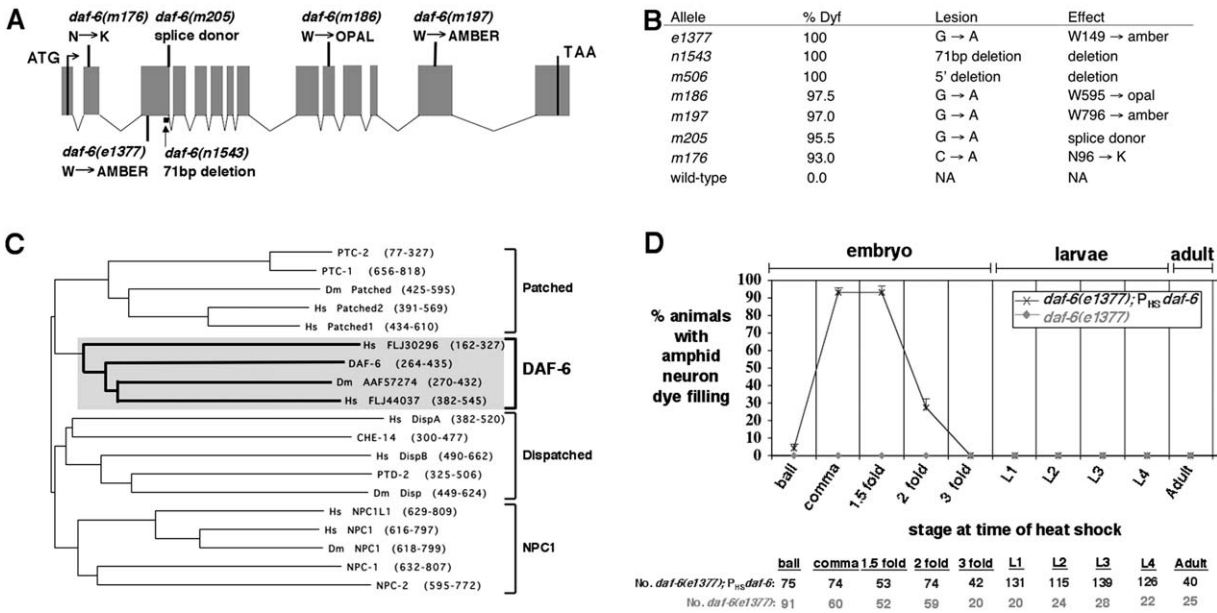


Figure 2. *daf-6* Encodes a Patched-Related Protein

(A) *daf-6* gene structure. Boxes, exons; V-shaped lines, introns. Mutation sites and nucleotide and mRNA/protein alterations are indicated. Putative null and hypomorphic mutations are below and above the gene schematic, respectively. The putative null allele *daf-6(m506)* lacks most of the 5' end of the gene and is not shown.

(B) Dye-filling defects (Dyf) per animal and molecular lesions of *daf-6* alleles. 200 animals were scored for each allele. NA, not applicable.

(C) Dendrogram showing sequence relationships of DAF-6 SSD to SSDs of related *C. elegans*, *Drosophila*, and human PTRs, Patched, Dispatched, and NPC1.

(D) Heat shock rescue of *daf-6* dye-filling defect by *daf-6* cDNA. Horizontal axis, time of heat shock; vertical axis, % animals with amphid neuron dye filling 4 days after heat shock; error bars, standard error of the mean (SEM). Numbers of animals assayed for each time point are indicated.

mine the location and nature of molecular lesions associated with each of the seven known *daf-6* alleles, we determined the sequences of all exons and exon/intron boundaries of *ptr-7* in each *daf-6* allele (Figure 2A). Amphid neurons in animals homozygous for either the *e1377*, *n1543*, or *m506* alleles were completely defective in dye uptake, and the remaining four alleles still conferred some ability to take up dye from the environment (Figures 2A and 2B).

A 2968 bp full-length *daf-6* cDNA clone was obtained from Yuji Kohara (DNA Data Bank of Japan). The *daf-6* intron/exon organization was determined by comparing the cDNA and genomic sequences (Figure 2A). Conceptual translation of the *daf-6* cDNA suggested that *daf-6* encodes a 913 amino acid protein similar to the Hedgehog receptor Patched and is one of 24 such *ptr* (patched related) genes in the *C. elegans* genome (Kuwabara et al., 2000; Kuwabara and Labouesse, 2002). All PTR proteins contain a sterol-sensing domain (SSD), a conserved 180 amino acid sequence predicted to form five transmembrane domains (Kuwabara and Labouesse, 2002). While other SSD-containing proteins are important regulators of development or metabolic homeostasis, no function has been assigned to PTR proteins.

DAF-6 and other PTR proteins are most closely related to the Patched, Dispatched, and NPC1 SSD-containing proteins, and the similarity to these proteins is greatest within the putative SSDs (Supplemental Figure

S1). Like Patched and Dispatched, DAF-6 contains 12 predicted transmembrane domains with large extracellular loops between transmembrane segments 1 and 2, and 7 and 8 (Kuwabara et al., 2000).

DAF-6 has potential *Drosophila* and human orthologs (Figure 2C; Supplemental Figure S1). Sequence comparisons suggest that these proteins are more closely related to DAF-6 than to other SSD-containing proteins (Figure 2C; Kuwabara et al., 2000). Thus, DAF-6 seems to belong to a conserved, previously uncharacterized, subfamily of SSD-containing proteins.

***daf-6* Is Required during Amphid Lumen Formation**

To further characterize the role of *daf-6* in amphid lumen formation, we sought to determine when *daf-6* function was required during development. We attempted to rescue the dye uptake defect of *daf-6(e1377)* animals at specific stages of development using a heat-inducible promoter (P_{HS}) to drive expression of the *daf-6* cDNA. *daf-6(e1377)* animals harboring an extrachromosomal array bearing the $P_{HS}daf-6$ transgene were incubated at 35°C for 30 min and assayed for dye uptake 4 days later. As shown in Figure 2D, expression of the *daf-6* cDNA at either the comma or 1.5-fold stages of embryogenesis corrected the dye uptake defect. Transgenic animals kept at 20°C, as well as nontransgenic *daf-6(e1377)* animals subjected to a heat shock, remained dye-filling defective (Figure 2D). Thus, *daf-6* functions around the comma and 1.5-fold stages of

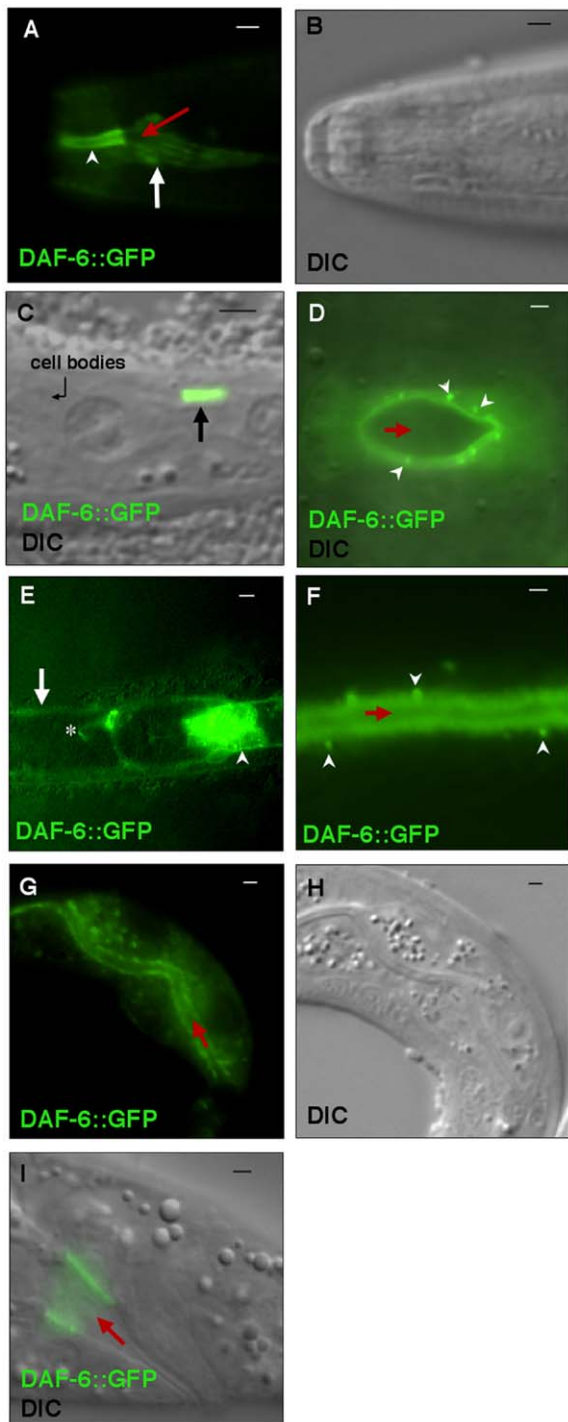


Figure 3. DAF-6 Lines the Luminal Surfaces of Tubes

All images are of wild-type animals expressing $P_{daf-6}daf-6::GFP$. (A and B) Fluorescence (A) and DIC (B) images of DAF-6::GFP localized to the amphid channel in an L2. White arrow, luminal surfaces of amphid sheath cell; arrowhead, amphid socket lumen; red arrow, sheath cell lumen. (C) Merged fluorescence and DIC image. DAF-6::GFP localized to phasmid sheath and socket cell channels (straight arrow). (D) Merged ventral fluorescence and DIC images of DAF-6::GFP in the vulva. GFP lines the lumen (red arrow) and localizes to puncta (arrowheads). (E) Fluorescence image (dorsal view). DAF-6::GFP lines lumen surfaces of the excretory canal cell (arrow), duct and pore cells (asterisk), gland cells (arrowhead). (F) Fluorescence image. DAF-6::GFP lines the excretory canal lumen (red arrow) and is seen in puncta (arrowheads). (G and H) Fluorescence (G) and DIC (H) images. DAF-6::GFP lines luminal surface of posterior intestine. Red arrow, lumen. (I) Merged fluorescence and DIC image. DAF-6::GFP localized to the luminal surface of K, K', F, and U cells. Red arrow, rectal lumen. In all images, except (D) and (E), anterior is left, dorsal is up. Scale bars equal 1 μm (except [E], 5 μm).

embryogenesis to promote amphid lumen formation. Embryos of similar stages (330 and 430 min postfertilization) were previously sectioned for EM and photographed by N. Thompson, J. White, and J. Sulston (Sulston et al., 1983). In these sections, the amphid sheath glia channel was not present at 330 min but was fully formed by 430 min (M. Heiman and S.S., unpublished results). Therefore, *daf-6* functions in the amphid at the time of amphid lumen formation.

Heat shock-induced *daf-6* expression during comma stage still rescued the dye uptake defect of *daf-6(e1377)* animals 8 days after induction (data not shown), suggesting that *daf-6* is not required for lumen maintenance. Two additional results support this conclusion. First, heat-induced expression of *daf-6* at the ball stage of embryogenesis (Figure 2D) did not rescue *daf-6(e1377)* animals, even though expression induced at comma stage, approximately 3 hr later, could rescue the defect. This experiment suggests that DAF-6 protein may be unstable. Second, as described below, expression of a rescuing DAF-6::GFP fusion protein was rarely observed in the amphid beyond the L1 larval stage. Thus, *daf-6* is probably required for lumen formation, and not maintenance.

DAF-6 Lines the Luminal Surfaces of Tubes

To determine in which cells *daf-6* was expressed, we examined wild-type animals containing a transgene expressing GFP under the control of a 3 kb *daf-6* promoter fragment. $P_{daf-6}GFP$ was expressed in the amphid sheath glia (Figures 1G and 1I), consistent with previous mosaic analysis studies suggesting that *daf-6* functions cell autonomously in these cells (Herman, 1987). Expression was also seen in amphid socket cells (Figures 1G and 1I), the phasmid sensory organ sheath and socket cells, cells of the excretory system (the excretory canal, duct, pore, and gland cells), the vulval E and F cells, the K, K', F, and U rectal epithelial cells, and less frequently in posterior intestinal cells. These cells all form tubes, suggesting that *daf-6* might function not only in amphid channel opening, but also in lumen morphogenesis of a variety of different tubes.

We also determined the expression pattern and sub-cellular localization of a DAF-6::GFP fusion protein produced from a $P_{daf-6}daf-6::GFP$ transgene able to rescue the dye uptake defects of *daf-6(e1377)* mutants. In the amphid, DAF-6::GFP fusion protein expression usually persisted only up to the L1 larval stage, and the protein localized to the region of the amphid channel formed by the sheath and socket cells (Figures 3A and 3B), supporting a role for DAF-6 in tube formation. DAF-

6::GFP also localized to the luminal surfaces of tubes generated by other cells expressing *daf-6* (Figures 3C–3I). As in the amphid, expression in the phasmid sheath and socket cells usually did not persist beyond the L1 larval stage. Expression in vulval cells was usually restricted to the L4 larval stage, after the cells were generated and during or shortly after the vulval lumen was generated. Expression in the rectum and excretory system was observed throughout embryogenesis and larval development, but usually not during adulthood.

Several SSD-containing proteins have been shown to associate with intracellular vesicles (Kuwabara and Labouesse, 2002). Interestingly, DAF-6::GFP protein was detected in punctate structures within the cytoplasm of expressing cells. This localization was best seen in the vulva and in the excretory canal cell (Figures 3D and 3F). Thus, DAF-6 may localize to vesicles as well.

DAF-6 Mutations Affect Function and Subcellular Localization

To define regions important for DAF-6 function and subcellular localization, we established transgenic lines expressing different mutant versions of the DAF-6::GFP rescuing protein. Patched, Dispatched, and NPC1 proteins share sequence features with members of the resistance nodulation division (RND) family of prokaryotic permeases, which function as antiporters that confer resistance to drugs or heavy metals (Nies, 1995; Tseng et al., 1999). These proteins share an overall similarity in membrane topology and contain a GxxxD motif predicted to be important in permease function within their fourth and tenth transmembrane domains (Guan and Nakae, 2001; Ma et al., 2002; Taipale et al., 2002). Unlike Patched and Dispatched, DAF-6 protein contains only a single GxxxD motif in its putative tenth transmembrane region. Altering the conserved aspartate residue of this motif to either asparagine or alanine, as done previously for Dispatched (Ma et al., 2002), reduced but did not eliminate rescue. Intriguingly, localization of a fraction of these mutant DAF-6 proteins was perturbed (most easily assessed in vulval cells; Figures 4B and 4C). These results suggest that DAF-6, and perhaps Patched and Dispatched as well, is not likely to function as an RND permease, but that the GxxxD motif may contribute to the regulation of DAF-6 protein localization.

The SSD has also been suggested to regulate protein localization. For example, point mutations in the SSD disrupt the subcellular localization and function of mammalian SCAP and the function of *Drosophila* Patched (Hua et al., 1996; Martin et al., 2001; Strutt et al., 2001). To examine the role, if any, of the DAF-6 SSD, we established transgenic animals expressing DAF-6::GFP proteins containing mutations similar to those used to study the SCAP and Patched SSD. Surprisingly, these mutant proteins were still functional; however, the Gly321Arg mutation disrupted the subcellular localization of a fraction of the DAF-6::GFP proteins (Figures 4D and 4E). We had also identified a mutation near the putative signal sequence of DAF-6 that similarly disrupted subcellular localization without disrupting function (Figure 4F). We determined whether the combination of this mutation with the SSD mutations would

abolish function. As shown in Figures 4G and 4H, these double mutant proteins failed to rescue the *daf-6* dye-filling defect, confirming a functional role for the DAF-6 SSD in protein localization. Interestingly, DAF-6 SSD alone was not sufficient to confer appropriate DAF-6 function or subcellular localization, suggesting that function and localization are not determined entirely by this domain (Figure 4I).

Two of the mutants we examined demonstrated that the extracellular loops of DAF-6 protein are also essential for its function. First, deletion of the second extracellular loop (Figure 4J) abolished both DAF-6 function and localization. A similar deletion in *Drosophila* Patched resulted in a dominant, Hedgehog-insensitive allele (Briscoe et al., 2001). Second, the *daf-6(m176)* allele results in a missense mutation, converting asparagine 96 to lysine in the first extracellular loop. We established transgenic animals expressing a DAF-6::GFP protein containing the identical mutation. As with the endogenous mutant protein, the mutant DAF-6::GFP protein was only able to rescue the dye-filling defect in a small percentage of expressing animals (Figure 4K). Surprisingly, however, subcellular localization of DAF-6::GFP was not disrupted by this mutation. This result suggests that proper DAF-6 localization is not sufficient for DAF-6 function and that DAF-6 activity may be regulated by interaction with other proteins making contact with the first extracellular loop.

Our studies also suggest that DAF-6 protein makes specific contact with other proteins as it transits to the plasma membrane. Specifically, a DAF-6::DsRed fusion protein, which was restricted to a perinuclear structure, perhaps the Golgi, blocked amphid neuron dye-filling and caused amphid vacuole accumulation, as seen in *daf-6* mutants (Figure 4L, data not shown). These defects may have been caused by DsRed-induced aggregation of DAF-6, titrating factors with which the protein normally interacts.

Taken together, our mutagenesis studies have revealed important domains required for DAF-6 localization and function, have provided evidence against a role for this protein (and perhaps other family members) as a permease, and have defined a specific extracellular residue that may contact other proteins required for DAF-6 activity.

daf-6 Functions with *che-14* to Regulate Lumen Formation

daf-6 has several features in common with the *C. elegans* Dispatched gene *che-14*. *daf-6* and *che-14* mutants display similar amphid defects: *che-14* mutants are dye-filling defective, dauer defective, chemotaxis defective, and osmotic avoidance defective (Perkins et al., 1986). *che-14* mutants also appear to have amphid channel defects, and amphid sheath cells in these mutants accumulate matrix-containing vacuoles (Perkins et al., 1986; Michaux et al., 2000). Furthermore, *che-14* is expressed in the amphid and phasmid sheath and socket cells, the excretory system, the vulva, and the rectum (Michaux et al., 2000). Finally, CHE-14 is a SSD-containing protein.

Because of these similarities, and despite previous studies showing that Dispatched and Patched proteins

	Transgene	Lesion	%Dyf (n) [Transgene in <i>daf-6(e1377)</i>]	%Dyf (n) [Transgene in WT]	Subcellular Localization	Image
A		none	A: 35% (52) B: 40% (78)	A: 0% (100) B: 0% (40)	localized	
B		D817N	A: 32% (88) B: 45% (222) C: 56% (44)	A: 0% (80) B: 0% (80) C: 0% (40)	localized/ diffuse	
C		D817A	A: 100% (100) B: 77% (70) C: 78% (110)	A: 33% (92) B: 0% (36) C: 0% (36)	localized/ diffuse	
D		G321R	A: 52% (50) B: 44% (50) C: 32% (50)	A: 0% (50) B: 0% (22) C: 10% (100)	localized/ diffuse	
E		M431N	A: 13% (60) B: 44% (50) C: 46% (54)	A: 2% (50) B: 3% (80)	localized	
F		G18E	A: 50% (50)	N.D.	diffuse	
G		G18E G321R	A: 100% (52) B: 100% (40) C: 100% (40)	A: 0% (40) B: 3% (40) C: 0% (40)	diffuse	
H		G18E M431N	A: 100% (40) B: 100% (42) C: 100% (46)	A: 0% (50) B: 2% (50) C: 0% (50)	diffuse	
I		SSD alone	A: 100% (100) B: 100% (40) C: 100% (60)	A: 1% (292) B: 2% (109) C: 1% (100)	diffuse	
J		Δ Loop 2	A: 100% (70) B: 100% (140) C: 100% (80)	A: 1% (150)	diffuse	
K		N96K	A: 97% (282) B: 100% (94) C: 99% (80)	N.D.	localized	
L		S253P F568L	N.D.	A: 81% (104)	peri-nuclear	

Figure 4. Mutations in DAF-6 Affect Function and Subcellular Localization

Indicated transgenes were injected into *daf-6(e1377)* or wild-type animals to establish transgenic lines. Independent lines of the same transgene are indicated by "A:", "B:", "C:". Animals were assayed for amphid dye-filling defects (Dyf) per amphid to assess rescue and dominant effects of the transgenes. Subcellular localization of transgenic proteins was assayed in vulvae of L4 animals where visualization was easiest, except in (L), where localization in amphids is shown at the sheath and socket cell bodies (black arrows). Green arrow, region of DAF-6::GFP localization in wild-type animals. N.D., not determined. Scale bars equal 1 μ m (except [L], 5 μ m).

function in different cell types, we surmised that *daf-6* and *che-14* might interact genetically within the same cells. To examine this possibility, we generated *che-14(e1960); daf-6(e1377)*, *che-14(ok193); daf-6(e1377)*, and *che-14(e1960); daf-6(m176)* double mutant animals. *che-14(ok193)* is a large deletion that, like *daf-6(e1377)*, is likely to be a molecular null. *che-14(e1960)* is a splice-site mutant that is phenotypically indistinguishable from *che-14(ok193)*. Double mutant animals were severely egg-laying defective, often forming “bags of worms” as the embryos hatched inside the mother. For example, whereas 0/51 *daf-6(e1377)* and 0/64 *che-14(e1960)* adults were egg-laying defective, 96/98 *che-14(e1960); daf-6(e1377)* adults were egg-laying defective (Figure 5A). Consistent with our dye-filling studies, the egg-laying defect of *che-14(e1960); daf-6(e1377)* animals was more severe than that of *che-14(e1960); daf-6(m176)* animals (Figure 5A).

che-14; daf-6 double mutants were also severely defective in excretory system function, exhibiting either a characteristic rod-like L1 larval lethal phenotype (Rod) or a distinctive clear (Clr) phenotype. These phenotypes are caused by an accumulation of fluid in the animal, giving it a translucent appearance. For example, whereas 3/143 *daf-6(e1377)* and 9/57 *che-14(e1960)* animals displayed excretory defects, 78/86 *che-14(e1960); daf-6(e1377)* animals displayed such defects (Figure 5B). *che-14; daf-6* animals were also slightly more defecation defective than either single mutant alone, consistent with defects in the posterior intestine and in rectal cells (data not shown).

Taken together, these experiments suggest that *daf-6* and *che-14* interact genetically, perhaps functioning in concert to regulate lumen formation in a variety of tubular structures throughout the animal.

To examine lumen formation directly in double mutant animals, we examined the morphology of the excretory canal cell lumen in *che-14(e1960); daf-6(e1377)* animals containing a P_{vha-1} :GFP reporter transgene. *vha-1* is expressed in the excretory canal cell (Oka et al., 1997). In wild-type animals, a continuous and uniform lumen extended within the two canal cell processes to the posterior tip of the animal (Figures 5C and 5D). *che-14(e1960); daf-6(e1377)* double mutants, however, had obvious lumen defects. While the canal cell extended two processes to the posterior tip of the animal, the lumen often extended only part way through these processes (Figures 5E–5G). Thus, in these double mutants, it appeared as though formation of the lumen had been initiated, but not completed. In some animals, regions containing vesicles were observed within the canal processes. Anterior to these pockets, the lumen was generally intact; however, posterior to the pockets, regions lacking lumen were present. These results suggest that the abnormal vesicle accumulation may represent a lumen formation intermediate (Figure 5G).

In addition to lumen extension defects, excretory canals in some animals displayed regions with cystic features, reminiscent of *exc* (excretory canal abnormal) mutants (Buechner et al., 1999; Berry et al., 2003) and *erm-1* mutants (Gobel et al., 2004). Unlike *exc* and *erm-1* mutants, however, *daf-6; che-14* mutants predominantly exhibited lumen formation defects rather than cystic features. Thus, as in the amphid, where the sen-

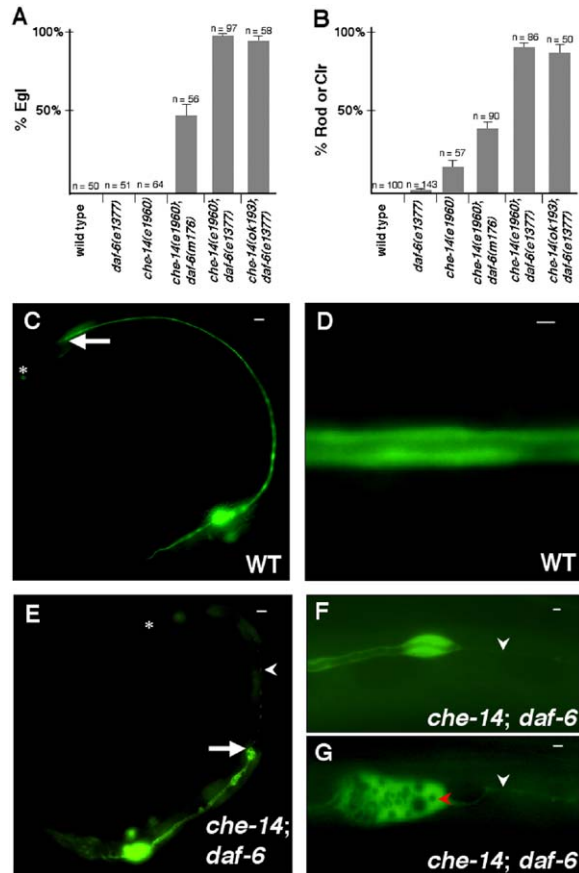


Figure 5. *daf-6* and *che-14* Interact to Regulate Lumen Morphogenesis

- (A) Histogram depicting egg-laying defects (Egl) of strains of the indicated genotype. Error bars, SEM.
 (B) Histogram depicting Rod and Clr defects (see text) of strains of the indicated genotype. Error bars, SEM.
 (C–G) Fluorescence images of animals expressing P_{vha-1} :GFP.
 (C) Wild-type animal. Excretory cell lumen (arrow) extends toward posterior end of the animal (asterisk).
 (D) Wild-type, note continuous lumen.
 (E) *che-14(e1960); daf-6(e1377)* mutant. Lumen fails to extend to posterior end of animal (arrow), but process does (arrowhead). Asterisk, posterior tip.
 (F) *che-14(e1960); daf-6(e1377)* mutant. Note lack of lumen in posterior region (arrowhead).
 (G) *che-14(e1960); daf-6(e1377)* mutant. Note lack of a lumen in posterior region (white arrowhead). Red arrowhead, numerous accumulated vesicles. In images (D), (F), and (G), anterior is left, dorsal is up. Scale bars equal 10 μ m in (C) and (E) and 1 μ m in (D), (F), and (G).

sory defects of *daf-6* mutants seemed to be due to a lumen formation defect in the sheath glia, the excretory dysfunction in *daf-6; che-14* double mutants appeared to result from a lumen formation defect in excretory system cells.

What is the nature of the genetic interaction between *daf-6* and *che-14*? Since both DAF-6 and CHE-14 are SSD-containing proteins, it is possible that both perform identical functions. If this were the case, overexpression of *daf-6* should rescue the defects of animals homozygous for a loss-of-function mutation in *che-14*.

To test this, we asked whether *che-14(1960)* animals carrying a P_{HS}*daf-6* transgene and subjected to a heat shock would remain defective for dye uptake. We found that overexpression of *daf-6* did not increase the frequency of amphid neuron dye filling. Specifically, 39/43 *che-14(e1960)*; P_{HS}*daf-6* animals heat-exposed at comma or 1.5-fold stages were dye-filling defective, and 69/91 *che-14(e1960)* nontransgenic heat-exposed comma or 1.5-fold embryos were defective in dye uptake. Animals heat-shocked at other stages of development also remained dye-filling defective. Conversely, overexpression of *che-14* using a P_{HS}*che-14* transgene able to rescue *che-14(e1960)* mutants did not rescue the dye-filling defect of *daf-6(e1377)* animals. Specifically, 66/66 *daf-6(e1377)*; P_{HS}*che-14* animals heat-exposed at comma or 1.5-fold stages were dye-filling defective. These results suggest that *daf-6* and *che-14* do not perform identical functions in the amphid.

We also examined whether DAF-6 was required for CHE-14 localization, and vice versa. We examined the subcellular localization of the proteins in the phasmid, because both *daf-6(e1377)* and *che-14(e1960)* were completely defective in dye uptake in this organ (Michaux et al., 2000). We found that DAF-6::GFP was still localized to the phasmid channel in *che-14(e1960)* mutants and that CHE-14::GFP was properly localized in *daf-6(e1377)* mutants (data not shown). Thus, localization of either protein was independent of the other.

Neuronal Cilia Are Important for Amphid Channel Morphogenesis

Since DAF-6 protein localizes to the amphid channel lumen, we reasoned that neuronal cilia residing in this lumen might directly or indirectly regulate DAF-6 function or localization. To test this idea, we examined the amphid channels of L1 animals homozygous for mutations in the *daf-19* gene and in which neuronal sensory cilia fail to form (Perkins et al., 1986; Swoboda et al., 2000). As with *daf-6* mutants, *daf-19* mutants accumulated vacuoles containing VAP-1::GFP within the sheath glia (Figures 6A and 6B). Matrix-filled vacuoles were also previously seen in EM cross-sections of *daf-19* mutants (Perkins et al., 1986). These results suggested that *daf-19* animals might harbor amphid channel defects that could, in part, be caused by abnormal DAF-6 function. To test this, we examined DAF-6::GFP localization in *daf-19* mutants. In wild-type animals, DAF-6::GFP localized to the lumen of the channel (Figures 6C, 6D, and 6G). In *daf-19(m86)* and *daf-19(m334)* mutants, however, DAF-6::GFP localized only to a punctate structure (Figures 6E–6G), approximately at the location of the junction between the sheath and socket channels. These defects were not due to a change in *daf-6* transcription within the sheath or socket glia (data not shown).

To confirm that altered DAF-6::GFP localization in *daf-19* mutants was indeed due to cilia defects, we also examined localization of this reporter protein in other cilia-defective mutants (Figure 6G). As in *daf-19* mutants, DAF-6::GFP in the amphid localized to a punctate structure in the cilia-defective mutants *che-3*, *che-11*, *che-13*, *daf-10*, and *osm-6*. Taken together, these results suggest that neuronal cilia regulate DAF-6::GFP localization in the amphid.

DAF-6::GFP appearance could be altered in cilia mutants either because cilia regulate DAF-6 localization or because cilia regulate sheath cell channel morphology. Previous EM analysis revealed no gross amphid channel defects in mutants with cilia defects (Perkins et al., 1986). Nevertheless, because DAF-6 localization was disrupted in these mutants, minor channel abnormalities might exist. To address this issue more rigorously, we examined the morphology of the channel in *daf-19* mutants. We examined serial cross-sections of two *daf-19(m86)* and three wild-type animals by EM. In 2/2 *daf-19(m86)* animals, we found a continuous lumen between the sheath and socket channels (four channels observed), and channel length was only mildly affected, if at all. Strikingly, however, the sheath channel lumen was irregular in shape, with branching outpockets (Figures 6H–6J). In addition, the distance from the anterior end of the dendrite to the anterior end of the sheath glia lumen was reduced in *daf-19(m86)* mutants (Figure 6J). Thus, altered DAF-6 localization in cilia-defective mutants may indeed lead to channel alterations. Alternatively, the absence of cilia in *daf-19* mutants may cause channel morphology defects independently of the DAF-6 localization defects.

Discussion

daf-6 Is Required for Lumen Morphogenesis

Several lines of evidence suggest that *daf-6* is required for lumen morphogenesis. Scanning EM (Albert et al., 1981), transmission EM, and fluorescent microscopy all revealed that *daf-6* sensory defects are due to a failure to generate a normal channel within the amphid sheath glia. In addition, *daf-6* functions cell autonomously in the sheath glia (Herman, 1987) and is required in the amphid during a narrow window of embryogenesis when the amphid sheath lumen forms. DAF-6::GFP localizes to the luminal surfaces of many tube-forming cells in *C. elegans*, including the amphid and phasmid sheath and socket cells, the excretory system, the vulva, the rectum, and the posterior intestine. Finally, all tubes containing DAF-6 protein are disrupted in *daf-6*; *che-14* double mutants.

What might be the role of *daf-6* in lumen formation? Vesicle fusion has been proposed to be a key step in lumen formation (Lubarsky and Krasnow, 2003). Luminal membrane surface is thought to be elaborated when vesicles fuse with this membrane. DAF-6::GFP was seen in punctate, vesicle-like structures (Figures 3D and 3F). Furthermore, *che-14*; *daf-6* double mutants accumulated unfused vesicles, instead of a lumen, in certain regions of the excretory canal (Figure 5G). Thus, DAF-6 may be involved in vesicle trafficking and may be specifically utilized to shuttle vesicles to or from growing lumina. Interestingly, lumen formation is topologically similar to cleavage furrow formation during cytokinesis. Specifically, generation and elongation of the cleavage furrow requires vesicle fusion with the plasma membrane (Straight and Field, 2000). The *C. elegans* Patched ortholog PTC-1, which is similar in sequence to DAF-6, may be required for vesicle transport during germ cell cytokinesis (Kuwabara et al., 2000). Thus, DAF-6, like PTC-1, may regulate vesicle dynamics during plasma membrane growth.

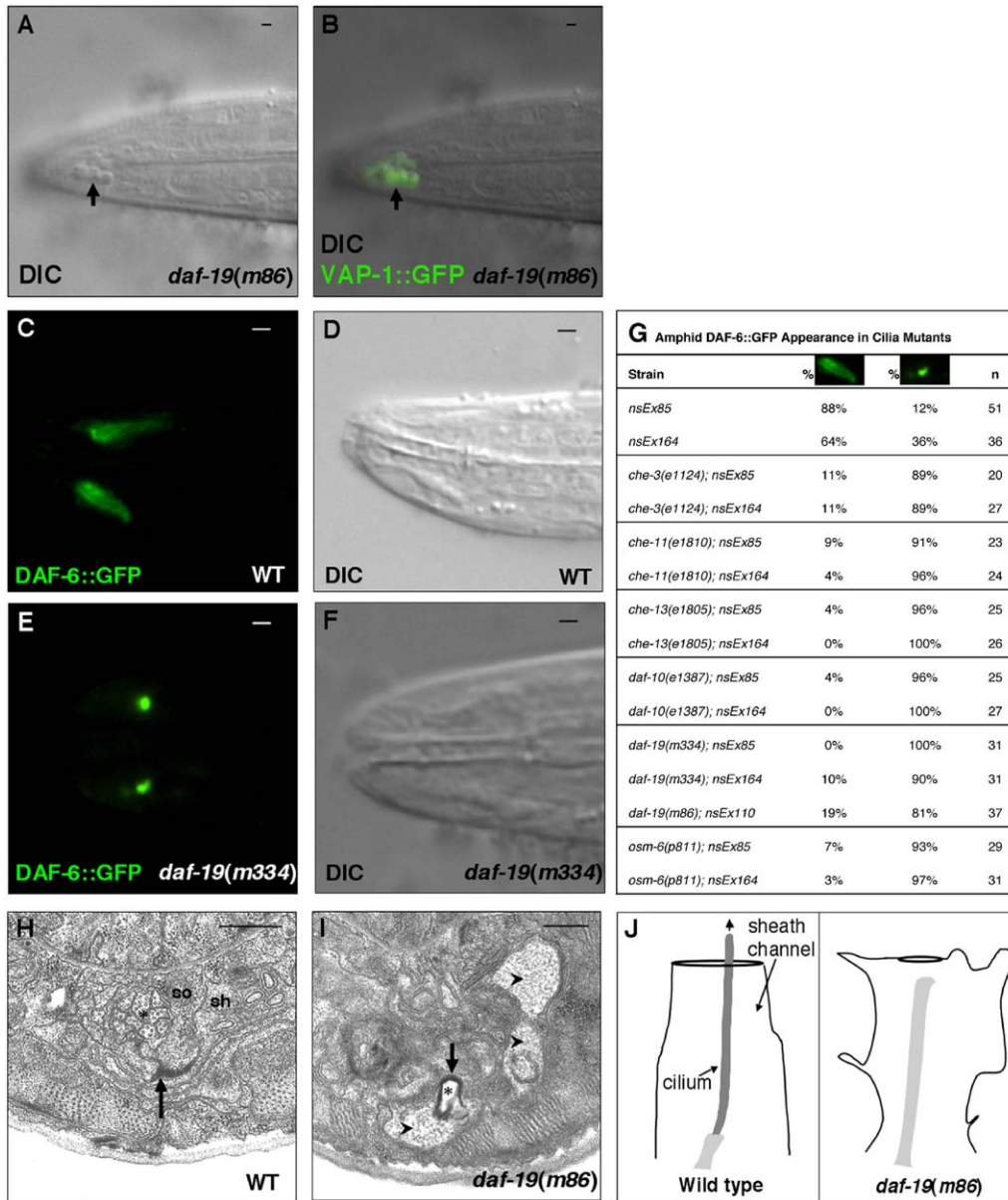


Figure 6. Defective Sheath Cell Lumen Morphogenesis in *daf-19* Mutants

(A and B) DIC (A) and merged fluorescence and DIC (B) images of a *daf-19(m86)* L1 expressing $P_{vap-1}::vap-1::GFP$. Arrows, matrix-filled vacuoles.

(C and D) Fluorescence (C) and DIC (D) images of a wild-type L1 expressing $P_{daf-6}::daf-6::GFP$.

(E and F) Fluorescence (E) and DIC (F) images of a *daf-19(m334)* L1 expressing $P_{daf-6}::daf-6::GFP$.

(G) Table charting DAF-6::GFP localization in strains of the indicated genotype. Each extrachromosomal array (*nsEx85*, *nsEx164*, *nsEx110*) is an independently generated $P_{daf-6}::daf-6::GFP$ transgene.

(H and I) Electron micrographs of the amphid sheath-socket junction (arrow) of a wild-type or *daf-19(m86)* L1, respectively. In (I), the junction is misshapen, and matrix-filled sheath pockets (arrowheads) are seen. so, socket; sh, sheath. Asterisks, amphid channel filled with cilia (H) or empty (I).

(J) Cartoons of amphid sheath channel in wild-type and *daf-19(m86)* animals based on electron micrographs of serially sectioned L1s. Only one dendrite is shown. In *daf-19(m86)* animals, the sheath-socket junction is misshapen, the amphid sheath channel is malformed, and the anterior end of the sensory dendrites are closer to the sheath-socket junction. (A)–(F) Dorsal images, anterior is left. Scale bars equal 1 μ m.

DAF-6 Is a Sterol-Sensing Domain-Containing Protein

Sequence comparisons suggest that DAF-6 is a member of a previously uncharacterized group of sterol-sensing domain (SSD)-containing proteins. How might

this observation explain the role of DAF-6 in lumen morphogenesis?

Seven protein subfamilies harbor SSDs (Kuwabara and Labouesse, 2002). Representatives of each subfamily include 7-Dehydrocholesterol reductase (Fitzky

et al., 1998), HMG CoA reductase (HMGCR) (Gil et al., 1985), SREBP cleavage activating protein (SCAP) (Hua et al., 1996), Neimann-Pick type C1 disease protein (NPC1) (Carstea et al., 1997), Dispatched (Burke et al., 1999), Patched (Hooper and Scott, 1989), and Patched-related (PTR) (Kuwabara et al., 2000) proteins. While these proteins have different activities, they can all be associated with vesicles, and the subcellular localizations of some, and perhaps all, are regulated through the SSD by sterol levels or by sterol-conjugated proteins (e.g., Hua et al., 1996; Nohturfft et al., 1999). Thus, the possible association of DAF-6 with vesicles is consistent with the localization of other SSD-containing proteins. Furthermore, our mutagenesis studies suggest that the DAF-6 SSD may help determine preferential DAF-6 localization to the plasma membrane.

Since PTR proteins are most closely related to Patched, could DAF-6, like Patched, function in a Hedgehog signal transduction pathway to generate tubes? In this pathway, Hedgehog protein inhibits the function of its receptor, Patched, resulting in activation of the membrane protein Smoothened. Smoothened activation allows nuclear entry of and transcription by the Gli/Ci transcription factor (Nybakken and Perrimon, 2002). It has been assumed that the Hedgehog signal transduction pathway does not exist in *C. elegans* (Kuwabara et al., 2000), because proteins similar in sequence to Smoothened have not been identified and because the *C. elegans* single Gli/Ci ortholog, *tra-1*, seems only to be involved in sex determination (Zarkower and Hodgkin, 1992). Furthermore, the *C. elegans* Patched homolog, *ptc-1*, functions in germline cytokinesis and probably does not function in a Hedgehog signal transduction pathway (Kuwabara et al., 2000). Nonetheless, our mutagenesis studies suggest that aspartate 96 of DAF-6, located in the first extracellular loop of the protein, is critical for DAF-6 function but not for localization, suggesting that this residue may interact with an extracellular protein to regulate lumen morphogenesis. There are several Hedgehog-like proteins encoded in the genome (Aspöck et al., 1999). Intriguingly, some of these are expressed in tube-forming cells (Aspöck et al., 1999). Thus, a rudimentary Hedgehog pathway might exist in *C. elegans* to control tube morphogenesis.

Our studies do not support the notion that DAF-6 acts as a permease for two reasons. First, DAF-6 harbors only a single GxxxD motif, unlike the two motifs present in the RND permeases. Second, mutations of this single GxxxD motif in DAF-6 did not fully block DAF-6 function, but did slightly affect protein localization, suggesting that reduced activity of these mutant proteins was due to mislocalization.

A Model for Amphid Lumen Formation

Our studies suggest that *daf-6* and *che-14* act in concert to regulate lumen formation in *C. elegans*. *che-14* is most similar to Dispatched, a protein required for the secretion of Hedgehog (Burke et al., 1999). Furthermore, previous studies suggested a role for CHE-14 in exocytosis (Michaux et al., 2000). *che-14* may, therefore, promote exocytosis during lumen formation. *daf-6* is similar to *Drosophila* and vertebrate Patched, and

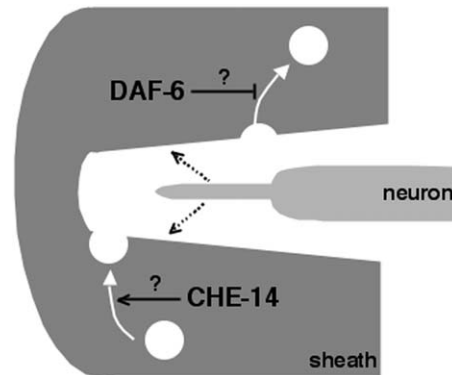


Figure 7. A Possible Model for Amphid Lumen Formation

A hypothetical developmental intermediate is shown. To generate the lumen and open the sheath glia channel, DAF-6 may inhibit endocytosis, while CHE-14 may promote exocytosis. DAF-6 and CHE-14 may act similarly in other tubes, such as the excretory canal. A signal from neuronal cilia (dashed arrow) may determine the shape of the amphid channel and DAF-6 localization.

binding of the Hedgehog ligand to Patched triggers endocytosis of the complex (Denef et al., 2000; Incardona et al., 2000; Martin et al., 2001; Strutt et al., 2001), an observation that led Michaux et al. (2000) to speculate that Patched-like proteins may be involved in endocytosis. One possible, although nonconventional, interpretation of this result is that the normal function of Patched is to inhibit endocytosis rather than promote it. Binding of Hedgehog to Patched would inhibit Patched activity, allowing endocytosis to occur. By analogy, we hypothesize that DAF-6 might function to inhibit endocytosis during lumen growth. Thus, we speculate that during lumen growth, more membrane is added to the growing lumen than is removed, by both promotion of exocytosis (using CHE-14) and inhibition of endocytosis (using DAF-6) (Figure 7).

Why do the posterior amphid channel and the excretory canal lumen still form in *daf-6* mutants? One possibility is that loss of DAF-6 would reduce inhibition of endocytosis; however, exocytosis by CHE-14 would still allow a channel to be generated. Loss of both DAF-6 and CHE-14 would, however, be predicted to result in a severely diminished ability to extend a lumen, as observed in the excretory canal. The variable expressivity of the excretory canal defect in *che-14*(null); *daf-6*(null) mutants suggests that even in this genetic background, lumen formation can take place. There are 23 additional Patched-related genes, as well as two Dispatched and three Patched genes in the *C. elegans* genome (Kuwabara et al., 2000). Some or all of these may also function in lumen formation. Thus, redundancy in both the inhibition of endocytosis and the promotion of exocytosis may lead to the relatively mild lumen morphogenesis defects in *daf-6* and *che-14* mutants.

The situation may be different during amphid channel opening. This process is topologically different from intracellular lumen formation (as in the excretory canal or the posterior amphid channel) or the generation of a lumen between two cells (as in the vulva and rectum). Amphid channel opening may require the generation of

a hole within a cell, and this process may be more sensitive to disruption of vesicle dynamics. We would propose, therefore, that since both *daf-6* and *che-14* single mutants manifest defects in amphid channel opening, both exocytosis and a lack of endocytosis may be necessary for this event to take place. Furthermore, little genetic redundancy must exist in this process. The fusion of lumina of different tracheal branches in *Drosophila* may occur by generating a hole through the cells, and this process may also involve vesicle trafficking (Samakovlis et al., 1996). Thus, proteins similar to DAF-6 and CHE-14 may also function in this and similar processes.

Finally, how is amphid channel morphogenesis coordinated to accommodate the neuronal cilia it ensheaths? Our studies of channel defects in animals with mutant neuronal cilia revealed two interesting findings. First, DAF-6::GFP was confined to a punctate structure near the sheath-socket junction. Second, the sheath glia portion of the channel was present but was misshapen in *daf-19* mutants. These results support a model in which cilia signal to the sheath glia to regulate the localization of DAF-6::GFP, which, in turn, regulates channel morphology (Figure 7). We envision a carefully controlled interplay between the neuronal endings and their associated glia, resulting in a well-patterned channel of appropriate dimensions. These results suggest that the amphid of *C. elegans* could be used as an exciting system in which to study glia-neuron interactions during nervous system development.

Experimental Procedures

General Methods and Strains

See Supplemental Data.

Dye Uptake and Heat Shock Assays

Dye Uptake

Animals were washed off NGM plates with M9 medium (Sulston and Hodgkin, 1988) and spun down briefly in a microfuge. The supernatant was removed, and the lipophilic dye 1, 1'-dioctadecyl-3, methylindodicarbocyanine, 4-chlorobenzenesulfonate salt ("DiD" solid; DiC₁₈(5) solid) (Molecular Probes) was added at 10 μ g/ml in M9. Animals were then soaked in dye for 2 hr in the dark and at room temperature. Animals were next placed on NGM plates seeded with *E. coli* strain OP50 and scored using a fluorescence dissecting microscope.

Heat Shock Studies

Animals were placed at 35°C for 30 min, allowed to recover at 20°C, and scored for dye uptake 4 or 8 days later.

Allele Sequence Determination

Coding region and intron/exon boundaries of *daf-6* were amplified by the polymerase chain reaction (PCR) from mutant animals using AmpliTaq DNA polymerase (Roche) and appropriate primers. Amplicons were sequenced using an ABI sequencer.

Plasmid Constructions

See Supplemental Data.

Germline Transformation

Germline transformations were carried out using standard protocols (Mello and Fire, 1995). Constructs were injected together with either plasmid pRF4, containing the dominant marker *rol-6(su1006)* (Mello et al., 1991), or plasmid pJM23, containing wild-type *lin-15* (Huang et al., 1994).

Microscopy

Animals were examined by epifluorescence using either a fluorescence dissecting microscope (Leica) or an Axioplan II compound microscope (Zeiss). Images were captured using an AxioCam CCD camera (Zeiss) and analyzed using the Axiovision software (Zeiss).

Electron Microscopy

Animals were fixed in 0.8% glutaraldehyde, 0.7% OsO₄, 0.1 M cacodylate buffer for 1 hr on ice. Samples were postfixed in 2% OsO₄, 0.1 M cacodylate buffer, mounted into agar blocks, dehydrated in a series of alcohols, and embedded in a mixture of Epon-Araldite. Thin sections (50 nm) were cut on an Ultracut E microtome, contrasted with 2% Uranyl Acetate and 1% Lead Citrate, and pictures were taken with a JEOL100 CX TEM at 80 kV.

Supplemental Data

Supplemental Data include a figure, a table, and Supplemental Experimental Procedures and can be found with this article online at <http://www.developmentalcell.com/cgi/content/full/8/6/893/DC1/>.

Acknowledgments

We thank Ann Baren, Dana Cruz, Glenn Gold, Dave Hall, Erika Hartwig, Bob Horvitz, and Helen Shio for EM assistance; Matthew Buechner, Oliver Hobert, Isao Katsura, Michel Labouesse, Don Riddle, Piali Sengupta, and the *Caenorhabditis* Genetics Center for strains; Max Heiman for the P_{vap-1}::GFP construct; Yuji Kohara for the *daf-6* cDNA; Marie-Anne Felix for vulval cell identification; Mark Schroeder and Simi Hinden for technical assistance; and Mary Abraham, Taulant Bacaj, Max Heiman, and Carine Waase for comments on the manuscript. This work was supported in part by funds from the Patterson Trust (to S.S.) and NIH MSTP grant GM07739 (to E.A.P.).

Received: July 19, 2004

Revised: January 19, 2005

Accepted: March 9, 2005

Published: June 6, 2005

References

- Albert, P.S., Brown, S.J., and Riddle, D.L. (1981). Sensory control of dauer larva formation in *Caenorhabditis elegans*. *J. Comp. Neurol.* 198, 435–451.
- Aspöck, G., Kagoshima, H., Niklaus, G., and Burglin, T.R. (1999). *Caenorhabditis elegans* has scores of hedgehog-related genes: sequence and expression analysis. *Genome Res.* 9, 909–923.
- Bargmann, C.I., and Mori, I. (1997). Chemotaxis and thermotaxis. In *C. elegans II*, D.L. Riddle, B.J. Meyer, and J.R. Priess, eds. (Cold Spring Harbor, NY: Cold Spring Harbor Laboratory Press), pp. 717–737.
- Bargmann, C.I., Hartwig, E., and Horvitz, H.R. (1993). Odorant-selective genes and neurons mediate olfaction in *C. elegans*. *Cell* 74, 515–527.
- Berry, K.L., Bulow, H.E., Hall, D.H., and Hobert, O. (2003). A *C. elegans* CLIC-like protein required for intracellular tube formation and maintenance. *Science* 5653, 2134–2137.
- Briscoe, J., Chen, Y., Jessell, T.M., and Struhl, G. (2001). A Hedgehog-insensitive form of Patched provides evidence for direct long-range morphogen activity of Sonic Hedgehog in the neural tube. *Mol. Cell* 7, 1279–1291.
- Buechner, M., Hall, D.H., Bhatt, H., and Hedgecock, E.M. (1999). Cystic canal mutants in *Caenorhabditis elegans* are defective in the apical membrane domain of the renal (excretory) cell. *Dev. Biol.* 214, 227–241.
- Burke, R., Nellen, D., Bellotto, M., Hafen, E., Senti, K.A., Dickson, B.J., and Basler, K. (1999). Dispatched, a novel sterol-sensing domain protein dedicated to the release of cholesterol-modified hedgehog from signaling cells. *Cell* 99, 803–815.

- Burkitt, H.G., Young, B., and Heath, J.W. (1993). *Wheater's Functional Histology* (Edinburgh, UK: Churchill Livingstone Press).
- Carstea, E.D., Morris, J.A., Coleman, K.G., Loftus, S.K., Zhang, D., Cummings, C., Gu, J., Rosenfeld, M.A., Pavan, W.J., Krizman, D.B., et al. (1997). Niemann-Pick C1 disease gene: homology to mediators of cholesterol homeostasis. *Science* *277*, 228–231.
- Davis, G.E., and Camarillo, C.W. (1996). An alpha 2 beta 1 integrin-dependent pinocytic mechanism involving intracellular vacuole formation and coalescence regulates capillary lumen and tube formation in three-dimensional collagen matrix. *Exp. Cell Res.* *224*, 39–51.
- Denef, N., Neubuser, D., Perez, L., and Cohen, S.M. (2000). Hedgehog induces opposite changes in turnover and subcellular localization of patched and smoothened. *Cell* *102*, 521–531.
- Driscoll, M., and Kaplan, J. (1997). Mechanotransduction. In *C. elegans II*, D.L. Riddle, B.J. Meyer, and J.R. Priess, eds. (Cold Spring Harbor, NY: Cold Spring Harbor Laboratory Press), pp. 645–677.
- Fitzky, B.U., Witsch-Baumgartner, M., Erdel, M., Lee, J.N., Paik, Y.K., Glossmann, H., Utermann, G., and Moebius, F.F. (1998). Mutations in the Delta7-sterol reductase gene in patients with the Smith-Lemli-Opitz syndrome. *Proc. Natl. Acad. Sci. USA* *95*, 8181–8186.
- Folkman, J., and Haudenschild, C. (1980). Angiogenesis in vitro. *Nature* *288*, 551–556.
- Fujiwara, M., Ishihara, T., and Katsura, I. (1999). A novel WD40 protein, CHE-2, acts cell-autonomously in the formation of *C. elegans* sensory cilia. *Development* *126*, 4839–4848.
- Ghabrial, A., Luschnig, S., Metzstein, M.M., and Krasnow, M.A. (2003). Branching morphogenesis of the *Drosophila* tracheal system. *Annu. Rev. Cell Dev. Biol.* *19*, 623–647.
- Gil, G., Faust, J.R., Chin, D.J., Goldstein, J.L., and Brown, M.S. (1985). Membrane-bound domain of HMG CoA reductase is required for sterol-enhanced degradation of the enzyme. *Cell* *41*, 249–258.
- Gobel, V., Barrett, P.L., Hall, D.H., and Fleming, J.T. (2004). Lumen morphogenesis in *C. elegans* requires the membrane-cytoskeleton linker *erm-1*. *Dev. Cell* *6*, 865–873.
- Guan, L., and Nakae, T. (2001). Identification of essential charged residues in transmembrane segments of the multidrug transporter MexB of *Pseudomonas aeruginosa*. *J. Bacteriol.* *183*, 1734–1739.
- Hedgecock, E.M., Culotti, J.G., Thomson, J.N., and Perkins, L.A. (1985). Axonal guidance mutants of *Caenorhabditis elegans* identified by filling sensory neurons with fluorescein dyes. *Dev. Biol.* *111*, 158–170.
- Herman, R.K. (1984). Analysis of genetic mosaics of the nematode *Caenorhabditis elegans*. *Genetics* *108*, 165–180.
- Herman, R.K. (1987). Mosaic analysis of two genes that affect nervous system structure in *Caenorhabditis elegans*. *Genetics* *116*, 377–388.
- Hooper, J.E., and Scott, M.P. (1989). The *Drosophila* patched gene encodes a putative membrane protein required for segmental patterning. *Cell* *59*, 751–765.
- Hua, X., Nohturfft, A., Goldstein, J.L., and Brown, M.S. (1996). Sterol resistance in CHO cells traced to point mutation in SREBP cleavage-activating protein. *Cell* *87*, 415–426.
- Huang, L.S., Tzou, P., and Sternberg, P.W. (1994). The *lin-15* locus encodes two negative regulators of *Caenorhabditis elegans* vulval development. *Mol. Biol. Cell* *5*, 395–411.
- Incardona, J.P., Lee, J.H., Robertson, C.P., Enga, K., Kapur, R.P., and Roelink, H. (2000). Receptor-mediated endocytosis of soluble and membrane-tethered Sonic hedgehog by Patched-1. *Proc. Natl. Acad. Sci. USA* *97*, 12044–12049.
- Jan, Y.N., and Jan, L.Y. (1993). The Peripheral Nervous System. In *The Development of Drosophila melanogaster*, M. Bate and A. Martinez Arias, eds. (Cold Spring Harbor, NY: Cold Spring Harbor Laboratory Press), pp. 1207–1244.
- Kuwabara, P.E., and Labouesse, M. (2002). The sterol-sensing domain: multiple families, a unique role? *Trends Genet.* *18*, 193–201.
- Kuwabara, P.E., Lee, M.H., Schedl, T., and Jefferis, G.S. (2000). A *C. elegans* patched gene, *ptc-1*, functions in germ-line cytokinesis. *Genes Dev.* *14*, 1933–1944.
- Lubarsky, B., and Krasnow, M.A. (2003). Tube morphogenesis: making and shaping biological tubes. *Cell* *112*, 19–28.
- Ma, Y., Erkner, A., Gong, R., Yao, S., Taipale, J., Basler, K., and Beachy, P.A. (2002). Hedgehog-mediated patterning of the mammalian embryo requires transporter-like function of dispatched. *Cell* *111*, 63–75.
- Martin, V., Carrillo, G., Torroja, C., and Guerrero, I. (2001). The sterol-sensing domain of Patched protein seems to control Smoothened activity through Patched vesicular trafficking. *Curr. Biol.* *11*, 601–607.
- Mello, C., and Fire, A. (1995). DNA transformation. *Methods Cell Biol.* *48*, 451–482.
- Mello, C.C., Kramer, J.M., Stinchcomb, D., and Ambros, V. (1991). Efficient gene transfer in *C. elegans*: extrachromosomal maintenance and integration of transforming sequences. *EMBO J.* *10*, 3959–3970.
- Michaux, G., Gansmuller, A., Hindelang, C., and Labouesse, M. (2000). CHE-14, a protein with a sterol-sensing domain, is required for apical sorting in *C. elegans* ectodermal epithelial cells. *Curr. Biol.* *10*, 1098–1107.
- Montesano, R., Schaller, G., and Orci, L. (1991). Induction of epithelial tubular morphogenesis in vitro by fibroblast-derived soluble factors. *Cell* *66*, 697–711.
- Mori, I., and Ohshima, Y. (1995). Neural regulation of thermotaxis in *Caenorhabditis elegans*. *Nature* *376*, 344–348.
- Myat, M.M., and Andrew, D.J. (2002). Epithelial tube morphology is determined by the polarized growth and delivery of apical membrane. *Cell* *111*, 879–891.
- Nies, D.H. (1995). The cobalt, zinc, and cadmium efflux system CzcABC from *Alcaligenes eutrophus* functions as a cation-proton antiporter in *Escherichia coli*. *J. Bacteriol.* *177*, 2707–2712.
- Nohturfft, A., DeBose-Boyd, R.A., Scheek, S., Goldstein, J.L., and Brown, M.S. (1999). Sterols regulate cycling of SREBP cleavage-activating protein (SCAP) between endoplasmic reticulum and Golgi. *Proc. Natl. Acad. Sci. USA* *96*, 11235–11240.
- Nybakken, K., and Perrimon, N. (2002). Hedgehog signal transduction: recent findings. *Curr. Opin. Genet. Dev.* *12*, 503–511.
- Oka, T., Yamamoto, R., and Futai, M. (1997). Three vha genes encode proteolipids of *Caenorhabditis elegans* vacuolar-type ATPase. Gene structures and preferential expression in an H-shaped excretory cell and rectal cells. *J. Biol. Chem.* *272*, 24387–24392.
- Perkins, L.A., Hedgecock, E.M., Thomson, J.N., and Culotti, J.G. (1986). Mutant sensory cilia in the nematode *Caenorhabditis elegans*. *Dev. Biol.* *117*, 456–487.
- Riddle, D.L., and Albert, P.S. (1997). Genetic and environmental regulation of dauer larva development. In *C. elegans II*, D.L. Riddle, B.J. Meyer, and J.R. Priess, eds. (Cold Spring Harbor, NY: Cold Spring Harbor Laboratory Press), pp. 739–768.
- Riddle, D.L., Swanson, M.M., and Albert, P.S. (1981). Interacting genes in nematode dauer larva formation. *Nature* *290*, 668–671.
- Samakovlis, C., Manning, G., Steneberg, P., Hacohen, N., Cantera, R., and Krasnow, M.A. (1996). Genetic control of epithelial tube fusion during *Drosophila* tracheal development. *Development* *122*, 3531–3536.
- Starich, T.A., Herman, R.K., Kari, C.K., Yeh, W.H., Schackwitz, W.S., Schuyler, M.W., Collet, J., Thomas, J.H., and Riddle, D.L. (1995). Mutations affecting the chemosensory neurons of *Caenorhabditis elegans*. *Genetics* *139*, 171–188.
- Straight, A.F., and Field, C.M. (2000). Microtubules, membranes and cytokinesis. *Curr. Biol.* *10*, 760–770.
- Strutt, H., Thomas, C., Nakano, Y., Stark, D., Neave, B., Taylor, A.M., and Ingham, P.W. (2001). Mutations in the sterol-sensing domain of Patched suggest a role for vesicular trafficking in Smoothened regulation. *Curr. Biol.* *11*, 608–613.
- Sulston, J., and Hodgkin, J. (1988). *Methods*. In *The Nematode Caenorhabditis elegans*, W.B. Wood, ed. (Cold Spring Harbor, NY: Cold Spring Harbor Laboratory Press), pp. 587–606.

Sulston, J.E., Schierenberg, E., White, J.G., and Thompson, J.N. (1983). The embryonic cell lineage of the nematode *Caenorhabditis elegans*. *Dev. Biol.* 100, 64–119.

Sutherland, M., Westlund, B., Burnam, L., Sluder, A., and Liu, L. (2001). Characterization of two *Caenorhabditis elegans* venom allergen-related proteins. Poster presentation, Mol (Taos, New Mexico: Helminth. Keystone Symp.).

Swoboda, P., Adler, H.T., and Thomas, J.H. (2000). The RFX-type transcription factor DAF-19 regulates sensory neuron cilium formation in *C. elegans*. *Mol. Cell* 5, 411–421.

Taipale, J., Cooper, M.K., Maiti, T., and Beachy, P.A. (2002). Patched acts catalytically to suppress the activity of Smoothened. *Nature* 418, 892–896.

Tseng, T.T., Gratwick, K.S., Kollman, J., Park, D., Nies, D.H., Goffeau, A., and Saier, M.H., Jr. (1999). The RND permease superfamily: an ancient, ubiquitous and diverse family that includes human disease and development proteins. *J. Mol. Microbiol. Biotechnol.* 1, 107–125.

Ward, S., Thomson, N., White, J.G., and Brenner, S. (1975). Electron microscopical reconstruction of the anterior sensory anatomy of the nematode *Caenorhabditis elegans*. *J. Comp. Neurol.* 160, 313–337.

Wegner, M. (2000). Transcriptional control in myelinating glia: the basic recipe. *Glia* 29, 118–123.

Yu, S., Avery, L., Baude, E., and Garbers, D.L. (1997). Guanylyl cyclase expression in specific sensory neurons: a new family of chemosensory receptors. *Proc. Natl. Acad. Sci. USA* 94, 3384–3387.

Zarkower, D., and Hodgkin, J. (1992). Molecular analysis of the *C. elegans* sex-determining gene *tra-1*: a gene encoding two zinc finger proteins. *Cell* 70, 237–249.